

Spectral and Temporal Shaping of Spectrally Incoherent Pulses in the Infrared and Ultraviolet

C. Dorrer and M. Spilatro

Laboratory for Laser Energetics, University of Rochester

Laser–plasma instabilities (LPI’s) hinder the interaction of high-energy laser pulses with targets. Simulations show that broadband, spectrally incoherent pulses can mitigate these instabilities. Optimizing laser operation and target interaction requires controlling the properties of these optical pulses. We demonstrate closed-loop control of the spectral density and pulse shape of nanosecond, spectrally incoherent pulses after optical parametric amplification in the infrared (~ 1053 nm) and sum–frequency generation to the ultraviolet (~ 351 nm) using spectral and temporal modulation in the fiber front end.¹ The high versatility of the demonstrated approaches can support the generation of high-energy, spectrally incoherent pulses by future laser facilities for improved LPI mitigation.

Temporal and spectral shaping are demonstrated on the fourth-generation laser for ultrabroadband experiments (FLUX) test bed, which is composed of a fiber front end, an optical parametric amplification (OPA) stage, a sum–frequency generation (SFG) stage, and a frequency-doubled Nd:YLF laser system generating the pump pulse for the OPA and SFG stage (Fig. 1). The fiber front end generates the broadband spectrally incoherent OPA seed and the coherent seed for the pump laser using a single high-bandwidth arbitrary waveform generator. The pump laser generates a sequence of two pulses to pump the OPA stage (second pulse) and the SFG stage (first pulse), with a relative delay set to compensate for the optical path difference at 1ω and 2ω between these two stages. Spectral shaping is implemented using a programmable filter (WaveShaper, II-VI). Temporal shaping is implemented using a Mach–Zehnder modulator (MZM) driven by a programmable arbitrary waveform generator (AWG70001, Tektronix).

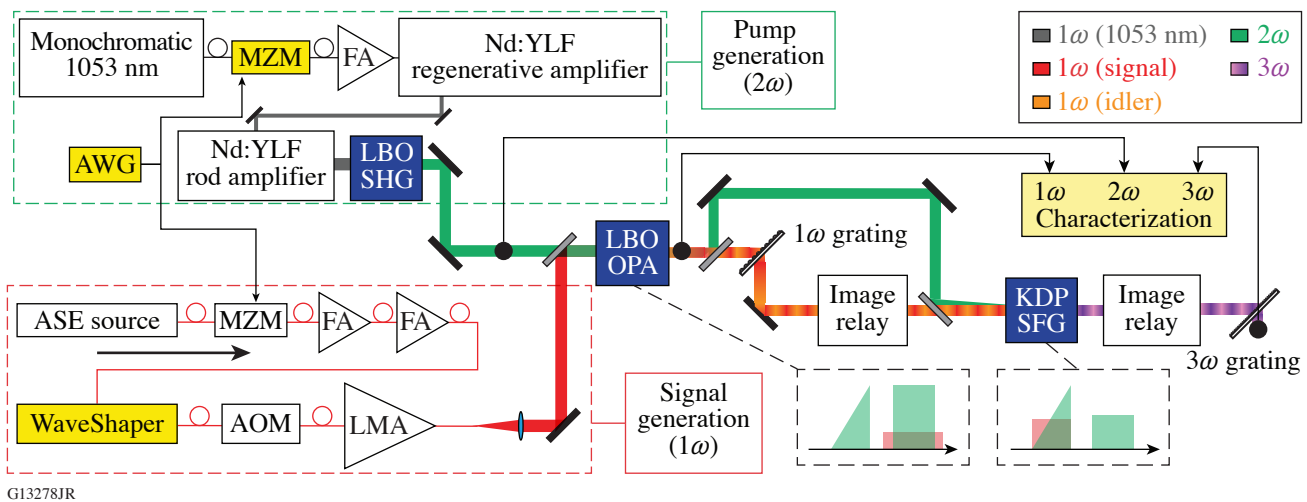


Figure 1

Experimental setup showing the signal generation at 1ω , pump generation at 2ω , amplification in the LBO OPA stage, and frequency conversion in the KDP SFG stage. The properties of the 1ω , 2ω , and 3ω pulses are measured after the OPA, SHG, and SFG stages, respectively. The insets represent the timing configuration for the 1ω pulse (in red) and the 2ω pulses (in green) within the OPA and SFG stages. SFG: sum frequency generation; SHG: sum-harmonic generation; ASE: amplified spontaneous emission; FA: fiber amplifier; AOM: acousto-optic modulator; LMA: large mode area.

The spectrum of the amplified signal measured after the OPA is shaped by controlling the spectrum of the input seed using the programmable spectral filter in the front end. Such shaping can precompensate the wavelength-dependent gain variations in the Yb-doped fiber amplifiers and OPA, although the latter are not expected to be significant, considering that a lithium triborate (LBO) OPA with that length has a bandwidth larger than 100 nm. Without spectral shaping, the OPA output spectrum peaks at ~ 1032 nm and has a full width at half maximum equal to 7 nm. The wavelength-dependent filter transmission is iteratively modified to decrease the error between the measured spectrum and target spectrum S_{target} (both peak-normalized to 1) using closed-loop control following

$$T_{n+1}(\lambda) = T_n(\lambda) + \eta[S_n(\lambda) - S_{\text{target}}(\lambda)], \quad (1)$$

where T_n and S_n are the transmission and spectrum as a function of wavelength λ at iteration n , respectively. For stability, the feedback is implemented with η typically equal to -0.1 . Initial conditions correspond to a fully transmissive spectral filter [$T_0(\lambda) = 1$] and the resulting spectrum $S_0(\lambda)$. The wavelength axes of the spectral filter and spectrometer are precisely mapped by generating and measuring narrow Gaussian spectra. Figure 2 presents spectral-shaping examples for which S_{target} has been set to a 10-nm flattop profile with a central wavelength ranging from 1032 to 1044 nm [Figs. 2(a)–2(d)] and to the same flattop profiles modulated by a parabolic term [Figs. 2(e)–2(h)]. This simulates spectral shaping for operation at different central wavelengths with precompensation of spectral gain narrowing in subsequent amplifiers.

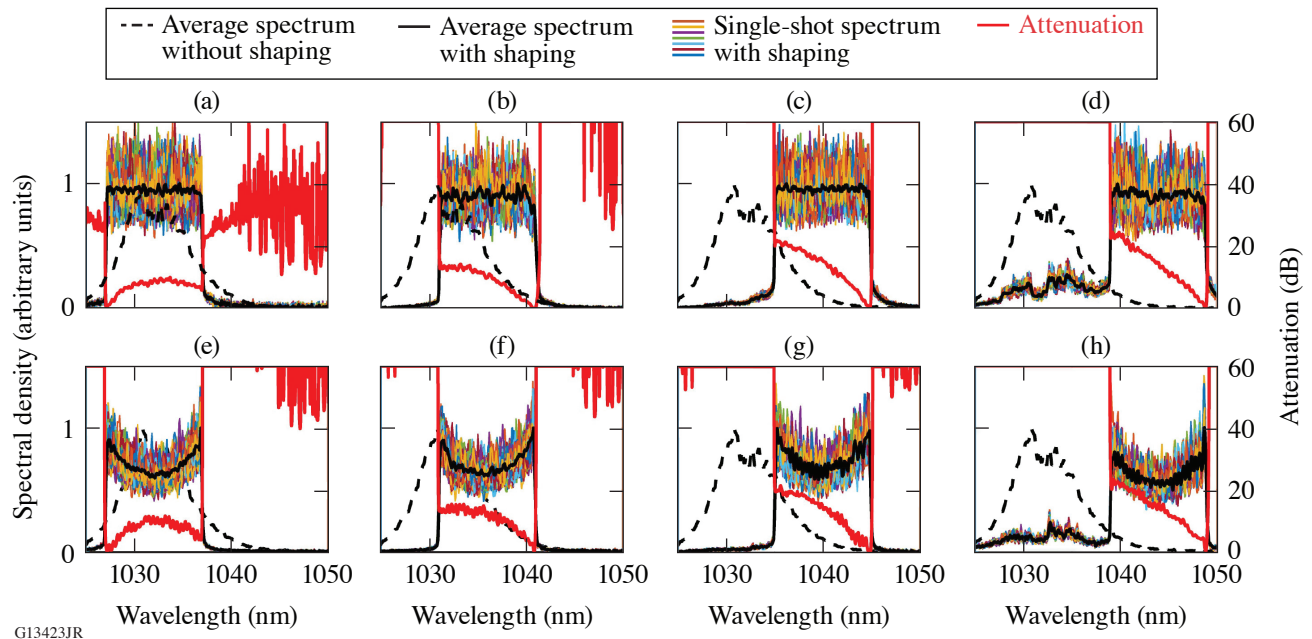


Figure 2

Spectral shaping of the OPA output signal. In the first row, S_{target} is a 10-nm flattop spectrum centered at (a) 1032, (b) 1036, (c) 1040, and (d) 1044 nm. In the second row [(e)–(h)], S_{target} is set to a 10-nm flattop spectrum with parabolic modulation centered at the same wavelengths. In all plots, the spectra averaged over 100 acquisitions without and with shaping are plotted using a dashed black line and solid black line, respectively. The spectra acquired over 100 successive shots are plotted with thin colored lines. The transmission of the spectral filter, in dB, is plotted with a thick red line.

The spectrally shaped 1ω pulses from the OPA are converted to spectrally shaped 3ω pulses using SFG with a narrowband 2ω pulse in a noncollinear angularly dispersed geometry.² SFG with a monochromatic field translates the input field along the frequency axis; i.e., it leads to identical spectral features for the input 1ω wave and output 3ω waves if the spectral acceptance is large enough. Figure 3 compares the 1ω and 3ω spectra, where the two wavelength ranges have been set to cover the same frequency range. For Fig. 3(a), the spectral-filter transmission is constant, whereas closed-loop control with various target spectra

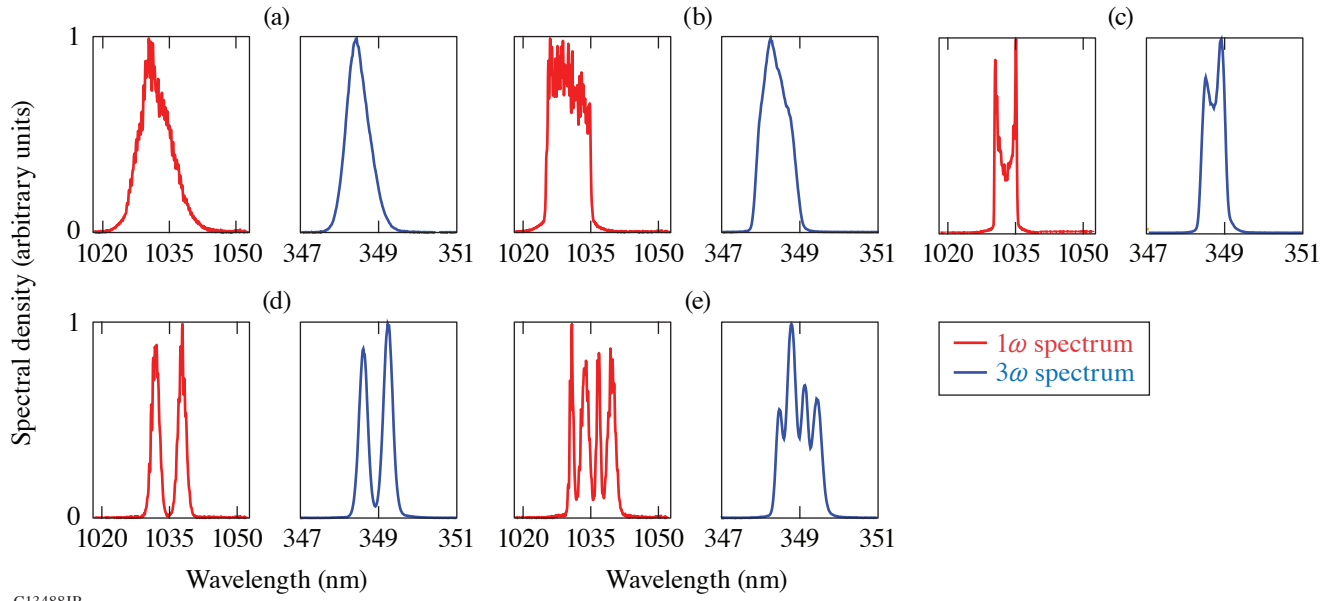


Figure 3

Spectral shaping of the SFG output signal corresponding to a shaped OPA output signal. Plots (a)–(e) show the 1ω spectrum (red line) and the 3ω spectrum (blue line), which are plotted over wavelength ranges that correspond to the same frequency span (10 THz).

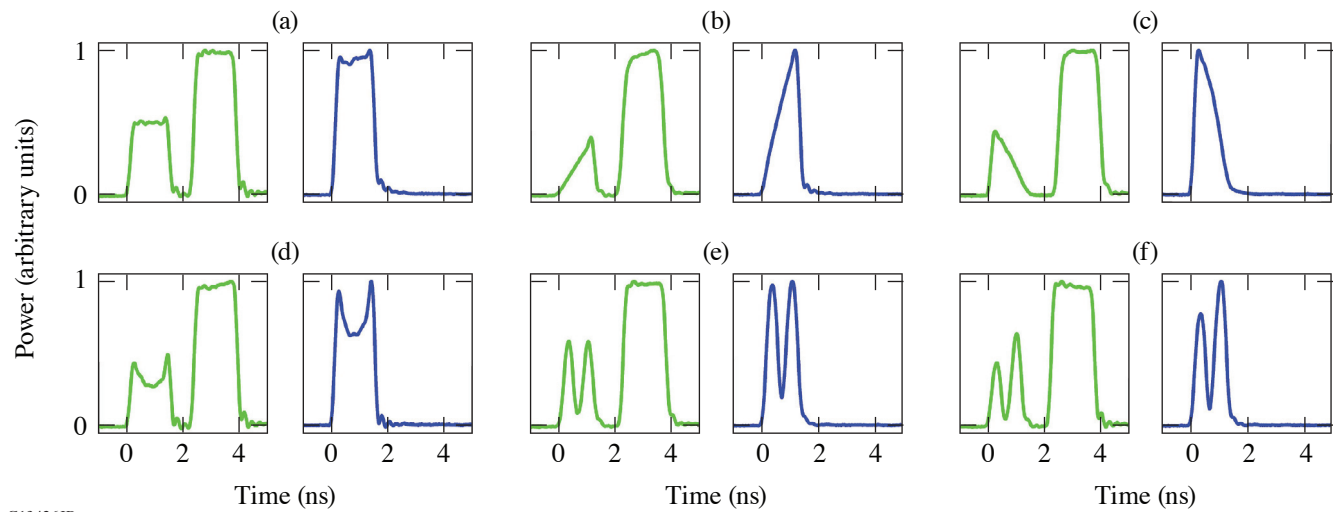
was used for the results shown in Figs. 3(b)–3(e). There is generally good agreement between the measured spectral shapes at 1ω and 3ω , although the latter have broader features because of the lower resolution of the UV spectrometer compared to the IR spectrometer (0.25 THz versus 0.05 THz).

Closed-loop pulse shaping has been implemented between the AWG-driven MZM in the fiber front end and the 2ω pulse shape after SHG. A preliminary calibration based on the generation of short Gaussian pulses at different times within the injection window of the regenerative amplifier maps out the linear relation between the time base of the AWG and oscilloscope. Saturation in the fiber amplifiers and Nd:YLF amplifiers leads to significant square-pulse distortion; i.e., the gain at earlier times is significantly higher than at later times within the pump pulse, while the gain observed at a given time depends on the energy that has been extracted at earlier times. Square-pulse distortion in the laser amplifiers, the nonlinear transfer function of the MZM relative to its drive voltage, and the nonlinear second-harmonic generation makes the temporal shaping of the output pulse a complex task. Closed-loop control to generate the pulse shape P_{target} is implemented as follows:

$$W_{n+1}(t) = W_n(t) + \eta [P_n(t) - P_{\text{target}}(t)], \quad (2)$$

where W_n and P_n are the time-dependent waveform and power at iteration n , respectively. The AWG and MZM are set to implement a monotonic relation between voltage and transmission, while operation at a reference voltage corresponds to the null transmission of the MZM. The shaped pulses, composed of the high-order super-Gaussian OPA pump pulse and the user-defined SFG pump pulse, are routed after convergence to the OPA and SFG stage. Figure 4 displays the shaped 2ω pulse and the resulting 3ω pulse for various user-defined profiles. A super-Gaussian OPA pump pulse (second pulse) is consistently obtained, allowing for temporally uniform OPA saturation. This leads to a flat-in-time amplified 1ω signal, and transfer of the SFG pump pulse shape (first pulse) from 2ω to 3ω via SFG.

This material is based upon work supported by the Department of Energy National Nuclear Security Administration under Award Number DE-NA0003856, the University of Rochester, and the New York State Energy Research and Development Authority.



G13426JR

Figure 4

Temporal shaping of the 2ω pump pulse (solid green line) and resulting 3ω pulse shape (solid blue line) for target profiles equal to (a) a super-Gaussian pulse, (b) a positive ramp, (c) a negative ramp, (d) a modulated super-Gaussian pulse, (e) a pair of short pulses with identical amplitudes, and (f) a pair of short pulses with unequal amplitudes. The 2ω pulse is composed of the SFG pump pulse (first pulse) and the OPA pump pulse (second pulse).

1. C. Dorrer and M. Spilatro, *Opt. Express* **30**, 4942 (2022).
2. C. Dorrer *et al.*, *Opt. Express* **29**, 16,135 (2021).